Regulation of TGF-β signaling and EMT in cancer progression

Zhang, J.

Chapter 5

Transforming growth factor-β challenge alters the *N*-, *O*-, and glycosphingolipid glycomes in PaTu-S pancreatic adenocarcinoma cells

Jing Zhang[1], Zejian Zhang[2,3], Stephanie Holst[2], Constantin Blöchl[2,4], Katarina Madunic[2], Manfred Wuhrer[2], Peter ten Dijke[1*] and Tao Zhang[2*]

[1]Oncode Institute and Dept. of Cell Chemical Biology, Leiden University Medical Center, 2300 RC Leiden, The Netherlands.

[2]Center for Proteomics and Metabolomics, Leiden University Medical Center, Leiden, The Netherlands.

[3]Current address: Department of Medical Research Center, Peking Union Medical College Hospital, Chinese Academy of Medical Sciences and Peking Union Medical College, Beijing, China

[4]Department of Biosciences, University of Salzburg, Salzburg, Austria.

Journal of Biological Chemistry. 2022 Feb 10;101717. doi: 10.1016/j.jbc.2022.101717.

Chapter 5

Abstract

Pancreatic ductal adenocarcinoma (PDAC) is characterized by poor prognosis and high mortality. Transforming growth factor-β (TGF-β) plays a key role in PDAC tumor progression, which is often associated with aberrant glycosylation. However, how PDAC cells respond to TGF-β and the role of glycosylation therein is not well known. Here, we investigated the TGF-β-mediated response and glycosylation changes in the PaTu-8955S (PaTu-S) cell line deficient in SMAD4, a signal transducer of the TGF-β signaling. PaTu-S cells responded to TGF-β by upregulating SMAD2 phosphorylation and target gene expression. We found that TGF-β induced expression of the mesenchymal marker N-cadherin, but did not significantly affect epithelial marker E-cadherin expression. We also examined differences in *N*-glycans, *O*-glycans, and glycosphingolipid (GSL) glycans in PaTu-S cells upon TGF-β stimulation. TGF-β treatment primarily induced *N*-glycome aberrations involving elevated levels of branching, core fucosylation, and sialylation in PaTu-S cells, in agreement with TGF-β-induced changes in the expression of glycosylation-associated genes. In addition, we observed differences in *O*- and GSL-glycosylation profiles after TGF-β treatment, including lower levels of sialylated Tn antigen and neo-expression of globosides. Furthermore, the expression of transcription factor SOX4 was upregulated upon TGF-β stimulation, and its depletion blocked TGF-β-induced *N*-glycomic changes. Thus, TGF-β-induced *N*-glycosylation changes can occur in a SOX4-dependent and SMAD4-independent manner in the pancreatic PaTu-S cancer cell line. Our results open up avenues to study the relevance of glycosylation in TGF-β signaling in SMAD4-inactivated PDAC.

Introduction

Pancreatic ductal adenocarcinoma (PDAC) is one of the most lethal tumors in the world. It is characterized by a poor prognosis and a failure to respond to therapy [1]. Genomic analysis of PDAC revealed that the most frequent genetic alterations include the activation of oncogene *KRAS* and inactivation of the tumor suppressors tumor protein p53 (*TP53*), Sma

and Mad related (*SMAD*) 4, and cyclin-dependent kinase inhibitor 2A (*CDKN2A*) [2-4]. The accumulation of these genetic mutations contributes to the stepwise progression of PDAC. *KRAS* mutations occur in the early stage of PDAC [5], whereas mutations of *TP53*, *SMAD4*, and *CDKN2A* arise in advanced pancreatic intraepithelial neoplasias and invasive pancreatic adenocarcinomas [6-8]. These common genetic abnormalities can profoundly perturb protein interactions and specific signaling pathways related to cell survival [9, 10], DNA damage repair [11], angiogenesis [12, 13], invasion [14], metastasis [15], and immune responses [16, 17].

The transforming growth factor-β (TGF-β) signaling pathway is involved in many cellular processes such as cell proliferation, apoptosis, migration, invasion, and immune evasion, contributing to various diseases, including cancer [18, 19]. TGF-β is a secreted cytokine for which cellular responses are initiated by binding to specific cell surface TGF-β type I and type II receptors, i.e., TβRI and TβRII. Upon TGF-β interaction with TβRII, TβRI is recruited, and a heteromeric complex is formed [20, 21]. Thereafter, the TβRII kinase phosphorylates the serine and threonine residues of TβRI, and thereby the extracellular signal is transduced across the plasma membrane [22]. Subsequently, intracellular signaling by TβRI proceeds via the phosphorylation of SMAD proteins, i.e., SMAD2 and SMAD3. Then, phosphorylated SMAD2/3 can form heteromeric complexes with the common SMAD mediator, i.e., SMAD4, which translocates into the nucleus to regulate the transcription of target genes [23]. SMAD4 is a critical mediator of TGF-β-induced growth arrest [24, 25] and apoptosis [26], which results in its role as a tumor suppressor at the early stages of cancer progression. However, the tumor-suppressive action of TGF-β/SMAD4 signaling is lost in nearly half of PDACs because of the inactivation of SMAD4 [27]. The SMAD4 gene deletion, frameshift mutation, or single point mutation can lead to the deficiency of functional SMAD4 protein, which further prevents or disrupts transduction of the canonical TGF-β/SMAD4 signaling pathway. Phosphorylated TGF-β receptors can activate SMAD2/3-dependent and SMAD4-independent pathways; in that case, receptor-regulated SMADs can make complexes with SRY-related HMG box 4 (SOX)4 or thyroid

transcription factor-1 (TTF-1, also known as NKX2-1), which compete with SMAD4 for interaction with SMAD3 [28, 29]. The SMAD3-TTF-1 and SMAD3-SOX4 complexes accumulate in the nucleus, regulate the expression of pro-oncogenic TGF-β target genes and induce tumorigenesis [28-31]. In addition, activated TβRI can signal via non-SMAD signaling pathways, such as the mitogen-activated protein kinase (MAPK) signaling cascade, including the extracellular signal-regulated kinase 1/2 (ERK1/2), c-Jun amino terminal kinase (JNK), p38, and other pathways like IκB kinase (IKK), phosphatidylinositol-3 kinase (PI3K)-AKT signaling as well as the Rho-like GTPase activity [32-36].

The SMAD-dependent and non-SMAD signaling pathways are involved in multiple cellular processes, including TGF-β-induced epithelial-to-mesenchymal transition (EMT) [37, 38]. EMT is a crucial step towards cell metastasis, during which the epithelial cells lose their polarity and cell-cell contacts and gain mesenchymal abilities such as enhanced migratory and invasive abilities [39]. EMT can be associated with morphological or phenotypic changes accompanied by a switch in the expression of EMT marker proteins, a loss of epithelial markers such as E-cadherin, claudin, and an increase of mesenchymal markers including N-cadherin, Vimentin, SNAIL, and SLUG [40, 41]. EMT is a dynamic and reversible process, and cells can undergo a complete EMT or, more commonly, take on a hybrid E/M status named “partial EMT”. The new term epithelial–mesenchymal plasticity (EMP) is used to describe the cells undergoing intermediate E/M phenotypic states [42]. Complete EMT and partial EMT both exist in PDACs, and the latter is speculated to be involved in collective cell migration and result in an enhanced metastasis rate through the formation of clusters of circulating tumor cells [43]. Recent studies have provided several mechanistic explanations for the TGF-β signaling in PDACs; for example, the restoration of SMAD4 in PDAC cells leads to a TGF-β-induced lethal EMT by triggering cell apoptosis via SOX4, indicating that EMT switches SOX4 function from pro-tumorigenic to pro-apoptotic [30].

Glycosylation of cellular proteins and lipids is a common post-translational modification in cells, which affects many cellular processes such as cell adhesion, proliferation, angiogenesis, migration, and invasion

[44, 45]. Dysregulated glycosylation is associated with TGF-β signaling and TGF-β-induced EMT in various cancers [46] by affecting the secretion, bioavailability of TGF-β [47], TβRII localization in cells, and interaction with TGF-β [48]. Moreover, specific glycan structures and glycogenes involved in the biosynthesis of *N*-glycans, *O*-glycans, and glycosphingolipid (GSL)-linked glycans always increase or decrease during TGF-β-induced EMT in various cancers [49] such as lung cancer [50] and breast cancer [49, 51]. During PDAC progression, aberrant glycosylation is highly correlated with several pathological processes [4, 52]. Several reports have demonstrated a number of glycosylation changes, including increased fucosylation and sialylation in pancreatic cancer progression in PDACs [53, 54]. The glycosylation changes of proteins such as mucin 5AC, insulin-like growth factor binding protein (IGFBP3), and galectin-3-binding protein (LGALS3BP) are involved in various signaling pathways, including TGF-β, tumor necrosis factor (TNF) and nuclear factor κ-light-chain-enhancer of activated B (NF-κ-B) pathways [55, 56]. In addition, the polypeptide *N*-acetylgalactosaminyltransferase 3 (GALNT3), one of the enzymes that catalyze the initial step in *O*-linked oligosaccharide biosynthesis, can promote the growth of pancreatic cells [57]. Moreover, some aberrations in glycosylation strongly influence the properties of tumor-associated extracellular matrix (ECM) and contribute to increased cell migration and invasion [58-61]. Indeed, the glycan-based cancer antigen (CA)-19-9 (sialyl Lewis A) has been recognized as the hallmark for the diagnosis and early detection of pancreatic cancer [62-65]. A better understanding of the aberrant glycosylation of PDAC induced by TGF-β may aid the identification of potential therapeutic targets and biomarkers. However, the underlying molecular mechanisms of TGF-β signaling in SMAD4-deficient PDAC cells and their relation to glycosylation are not well understood.

In this study, the PaTu-8988S (PaTu-S) cell line, a human epithelial-like PDAC cell line exhibiting KRAS activation and inactivation of SMAD4 and CDKN2A, was employed to investigate TGF-β responses and resulting glycosylation changes. Upon TGF-β treatment, PaTu-S cells were first analyzed for any effects on gene expression, morphological changes, loss of epithelial traits, and gain of mesenchymal markers. Next,

by combining transcriptomic analysis of glycosylation-associated genes with mass spectrometry glycomics, we systematically assessed the TGF-β-induced alterations in the three major classes of cell surface glycans of PaTu-S, namely, *N*-, *O*- and GSL-glycans. Furthermore, we investigated the critical role of SOX4 in TGF-β signaling and TGF-β-induced glycosylation in PaTu-S cells. This provides a stepping-stone for further studies on how glycosylation alterations contribute to TGF-β-mediated tumorigenesis of PDAC.

Results

TGF-β-induced responses in the PaTu-S cell line

To investigate whether the PaTu-S cell line, which lacks SMAD4, is responsive to TGF-β treatment (Figure S1A**)**, we performed Western blot analysis of phosphorylated SMAD2 levels of PaTu-S cells without and with TGF-β challenge. In PaTu-S cells, SMAD2 phosphorylation was significantly upregulated upon TGF-β stimulation for 1 h, which was blocked by treatment with TβRI kinase inhibitor SB431542 (Figure 1A). The expression of TGF-β target genes, including cellular communication network factor 2 (*CCN2*) [66, 67]*,* serpin family E member 1 (*SERPINE1*) [68, 69]*,* parathyroid hormone-like hormone (*PTHLH*) [70], and *SMAD7* [71] were induced by TGF-β treatment at multiple time points (Figure 1B). These genes can be induced by TGF-β/SMAD and non-SMAD pathways and in cells in which SMAD4 was inactivated [72]. In response to TGF-β stimulation for 2 days, the PaTu-S cells showed an upregulation in the expression of both the epithelial marker gene cadherin 1 (*CDH1*, encoding the protein E-cadherin) and the mesenchymal marker genes *CDH2* (encoding the protein N-cadherin)*,* SNAIL family transcriptional repressor 2 (*SNAI2*, encoding the protein SLUG) and *VIM* (encoding the protein vimentin) (Figure 1C). At the protein level, the mesenchymal marker N-cadherin was increased after TGF-β stimulation, whereas E-cadherin and SLUG expression levels were not significantly affected (Figure 1D). In addition, no morphological changes of PaTu-S cells were observed after 2 days of TGF-β treatment (Figure S1B) or even longer treatment times (data not shown). The response of PaTu-S cells to TGF-

β-treatment was further analyzed by immunofluorescence staining of E-cadherin and filamentous (F)-actin. We observed that TGF-β induced an

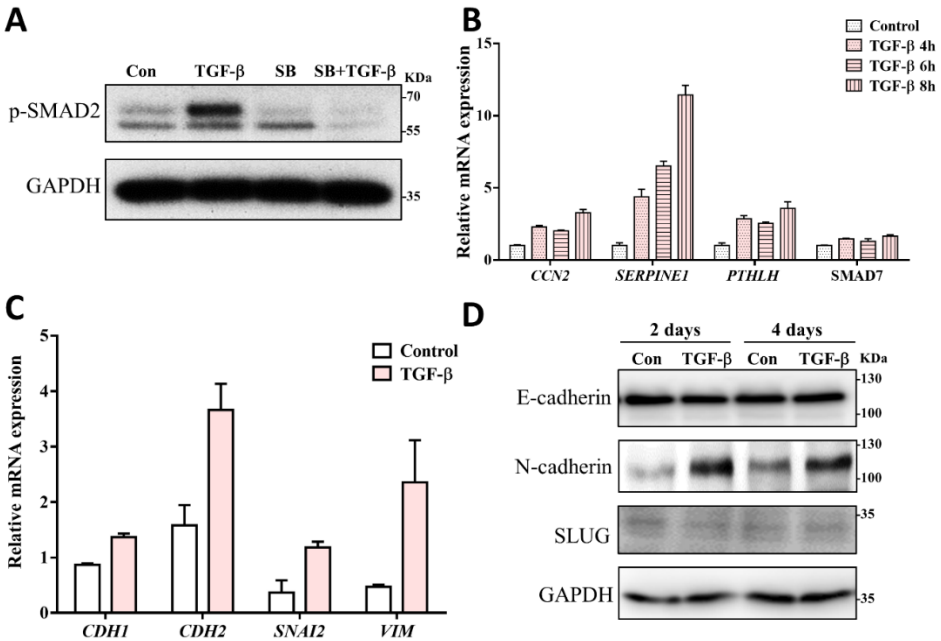

Figure 1. PaTu-S cell responses to TGF-β. (A) TGF-β-induced p-SMAD2 levels in PaTu-S cells by Western blot analysis. GAPDH, loading control. Cells were treated solely with vehicle control (Con) or TGF-β for 1 h. SB431542 (SB; 10 μM), a selective small molecule inhibitor of TGF-β type I receptor, was added for 2 h, 1 h treatment prior to TGF-β and then in combination with TGF-β for 1 h. **(B)** qRT-PCR analysis of TGF-β target genes, including CCN2, SERPINE1, PTHLH and SMAD7 in PaTu-S cells treated with vehicle control or TGF-β for 4, 6 and 8 h. GAPDH mRNA levels were used for normalization. **(C)** qRT-PCR analysis of epithelial and mesenchymal markers including CDH1, CDH2, SNAL2 and VIM in PaTu-S cells treated with vehicle control or TGF-β for 2 days. GAPDH mRNA levels were used for normalization. **(D)** E-cadherin, N-cadherin and SLUG levels by Western blot analysis in PaTu-S cells treated with vehicle control or TGF-β for 2 days and 4 days. In latter case, fresh medium containing TGF-β or vehicle control was added after 2 days. GAPDH, loading control. Molecular weight markers are indicated on the right. Three independent experiments were performed. Representative results are shown or the data is expressed as the mean ± s.d. (n=3). TGF-β was applied at final concentration of 2.5 ng/mL.

increase in the formation of lamellipodia and broadened and increased flat membrane protrusions at the leading edge of cells (Figure S1C). However, in response to TGF-β, no significant changes in E-cadherin expression and localization were observed. As an increase of lamellipodia formation has

been linked to an increase in cell migration [73], we next examined the TGF-β response of PaTu-S cells using an embryonic zebrafish xenograft extravasation model (Figure S1D, E). The PaTu-S cells were pre-treated with TGF-β or vehicle control for 2 days, and thereafter a similar number of cells were injected into the circulation of zebrafish embryos. After 4 days post-injection, we observed an increased number of invasive cell clusters (more than 5 cells in one cluster) in the caudal hematopoietic tissue (CHT) in the TGF-β pre-treatment group compared to the non-treated group. Thus, TGF-β pre-treatment promoted the extravasation of PaTu-S cells (Figure S1D, see representative images in Figure S1E). Taken together, these results indicate that the PaTu-S cells responded to TGF-β with an upregulation of SMAD2 phosphorylation and target gene expression. In addition, upon TGF-β treatment, an increase in mesenchymal marker expression was observed, but without a decrease or change in localization of epithelial markers. Moreover, TGF-β treatment of PaTu-S promoted the lamellipodia formation in vitro and cell extravasation in vivo.

Differential glycosylation of PaTu-S cells following TGF-β stimulation

Changes in glycosylation of lipids and cell surface proteins control various cellular pathways, including TGF-β signaling. Perturbations of these pathways are associated with pathological processes, i.e., cancer progression [46]. Prompted by our findings regarding the effects of TGF-β on PaTu-S cell behavior, we investigated the differential glycosylation of PaTu-S upon TGF-β treatment. We performed a comprehensive glycomic analysis of *N*-, *O*- and GSL-glycans. Cell pellets were divided into two parts: one for the analysis of *N*- and *O*-glycans [74], and the other for the analysis of GSL-glycans. For the analysis of all three glycan classes, we used PGC nano-LC-ESI-MS/MS in negative electrospray ionization mode, enabling the discrimination between glycan isomers [75, 76]. Glycan structures were assigned on the basis of the obtained LC-MS/MS data and general glycobiological knowledge, which are supplied in the supplementary information Figure S10 (*N*-glycan), S11 (*O*-glycan), S12 (GSL-glycan). Relative quantification of each glycan with and without TGF-β treatment was performed and summarized in Table S1 (*N*-glycan),

S2 (*O*-glycan) and S3 (GSL-glycan). Glycomic signatures were complemented by analyzing expression levels of glycosylation-associated genes in the cells. Glycan species, traits or ratios reflecting certain biosynthetic steps were calculated to facilitate the biological interpretation of the data and to relate the MS glycomics data to transcriptomics data.

Significant differences of *N*-glycosylation in PaTu-S cells with and without TGF-β-treatment

A total of 30 major *N*-glycan isomers spanning 27 different glycan compositions were manually identified from the investigated samples. In agreement with our previous work on *N*-glycan analysis of PaTu-S cell lines based on MALDI-TOF MS [77], the *N*-glycome data of PaTu-S was found to span 4 main *N*-glycan classes with major amounts of oligomannose (~47%) and complex type *N*-glycans (~39%), and lesser contributions of paucimannose (~10%) and hybrid type *N*-glycans (~4%) (Figure 2A). More than 39% of the *N*-glycans were fucosylated, and roughly 60% were sialylated. In addition, approximately 12% of oligomannose type *N*-glycans were phosphorylated. The complex *N*-glycans were primarily diantennary (~65%), with triantennary structures also present in significant amounts (~15%).

Upon TGF-β treatment, various *N*-glycosylation changes were observed. Complex *N*-glycans were increased and accounted for ~49% of the *N*-glycome after TGF-β treatment in contrast to ~39% in controls (Figure 2B). Specifically, triantennary *N*-glycans increased from ~14% to ~21% with TGF-β-treatment (Figure 2B), which is exemplified by the rather late-eluting, triantennary, trisialylated *N*-glycan species (Figure 2A). These data are in accordance with the significant upregulation of *N*-acetylglucosaminyltransferase (*MGAT*) *4A, MGAT4B,* and *MGAT5A* mRNA transcripts, 3 genes that encode enzymes involved in the synthesis of triantennary *N*-glycans, upon TGF-β treatment for 2 days and 4 days (Figure 2C, S2B). Notably, sialylation was high in PaTu-S cells after TGF-β treatment (0.9 sialic acid per glycan on average) with a relative abundance at ~90%, compared to ~60% under control conditions (Figure 2B), which is in line with the expression patterns of ST3 β-galactoside α-2,3-sialyltransferase (*ST3GAL*)*2*, *ST3GAL3*, *ST3GAL4*, and ST6 β-galactoside α-2,6-sialyltransferase 1 (*ST6GAL1)* (Figure 2C, S2B).

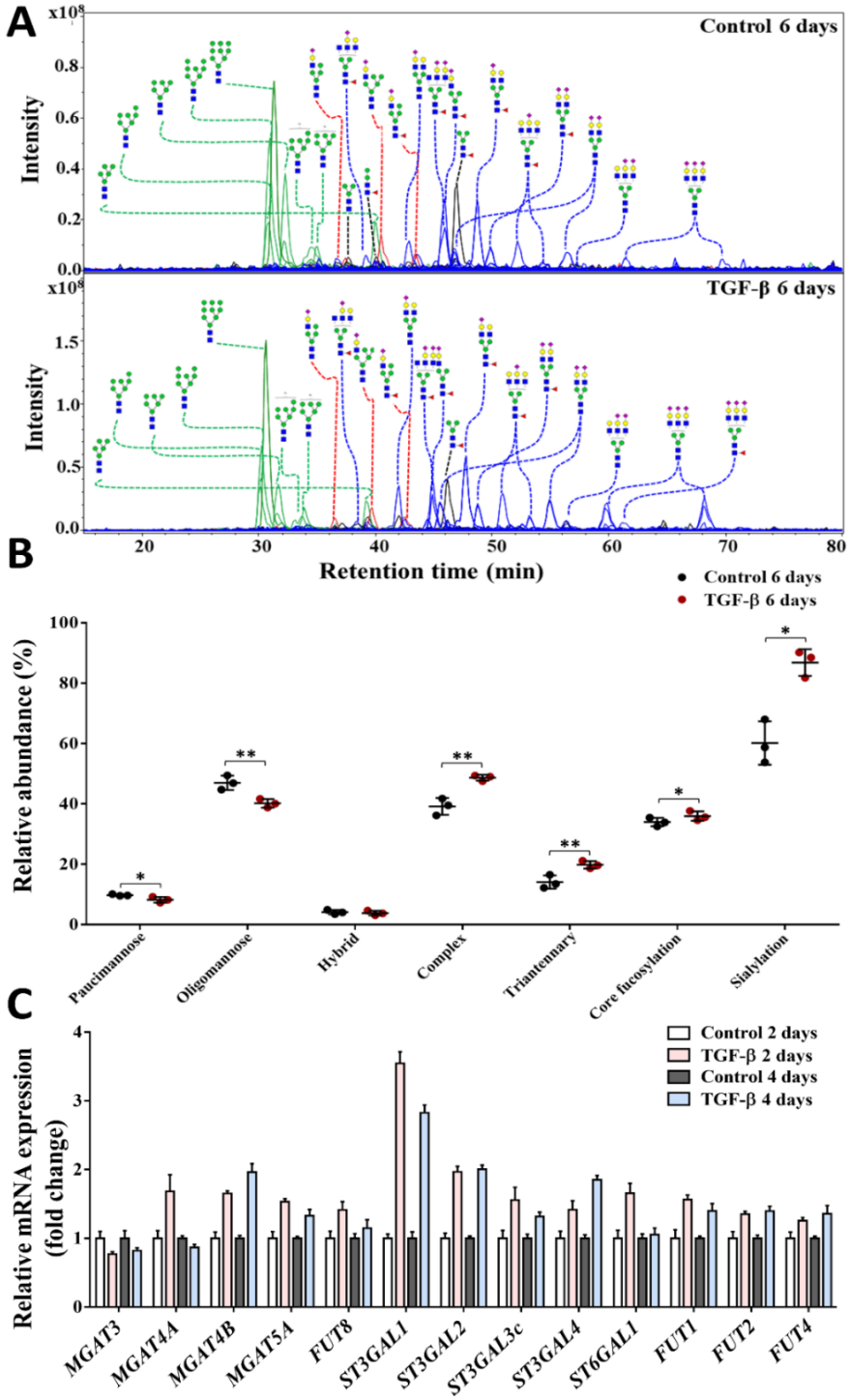

Figure 2. Differences of *N*-glycosylation in PaTu-S cell line with and without TGF-

β treatment. (A) Combined extracted ion chromatograms (EICs) of *N*-glycans were derived from PaTu-S cells treated with vehicle control or TGF-β for 6 days and analyzed by PGC nano-LC-ESI-MS/MS. Green trace: oligomannose; red trace: hybrid type; black trace: paucimannose; blue trace: complex type. **(B)** Relative abundance of *N*-glycan classes treated with or without TGF-β for 6 days. **(C)** qRT-PCR analysis of *N*-glycan-associated glycosyltransferases gene expression levels in PaTu-S cells treated with vehicle control or TGF-β for 2 days or 4 days. GAPDH was used for normalization to get the relative mRNA expression, and then gene expression levels in the control groups (2 days and 4 days) were used for further normalize the genes in TGF-β-treated groups (2 days and 4 days) to get fold changes data. Representative results are shown of three independent experiments, or the data is expressed as the mean ± s.d. (n=3). *P ⩽ 0.05, **P ⩽ 0.01, ***P ⩽ 0.001. Fresh medium with TGF-β (2.5 ng/mL) or vehicle control was added every 2 days in all experiments.

In addition, a slightly higher level of core fucosylation was observed (Figure 2B), in line with the upregulation of fucosyltransferase 8 (*FUT 8*) (Figure. 2C, S2B). Moreover, TGF-β treatment induced a decrease of oligomannose *N*-glycans from ~47% to ~39% in the PaTu-S cell line (Figure 2B). For a complete overview of the glycan quantification data and glycosylation-associated gene expression levels, see Figure S2.

Differences of *O*-glycosylation in PaTu-S cells with and without TGF-β-treatment

Following the *N*-glycan analysis, we analyzed 22 *O*-glycan species spanning 16 glycan compositions with relative quantification (Figure S3A**)**. The *O*-glycans mainly consisted of core 1 (~52%) and core 2 structures (~41%), with low levels of core 4 structures also present (~2%). A high level of sialylation (more than 97%) was observed in PaTu-S-derived *O*-glycans, while roughly 2% of the structures were fucosylated.

The *O*-glycan profiles were very similar in TGF-β-treated PaTu-S cells and non-treated cells (Figure 3A), showing a few minor and consistent changes. An increase in core 1 *O*-glycans was observed together with a decrease in core 2/4 *O*-glycans (Figure 3B), probably resulting from the significant upregulation of *C1GALT1* and *GCNT3* (Figure 3C, S3B). A lower level of sialyl Tn antigen was detected upon TGF-β treatment (Figure 3B), which is in line with the slightly decreased *ST6GALNAC1* (Figure 3C, S3B). For sialylation, a significant increase of α2,3 sialylation of galactose from 55% to 62% was observed (Figure 3B) in accordance

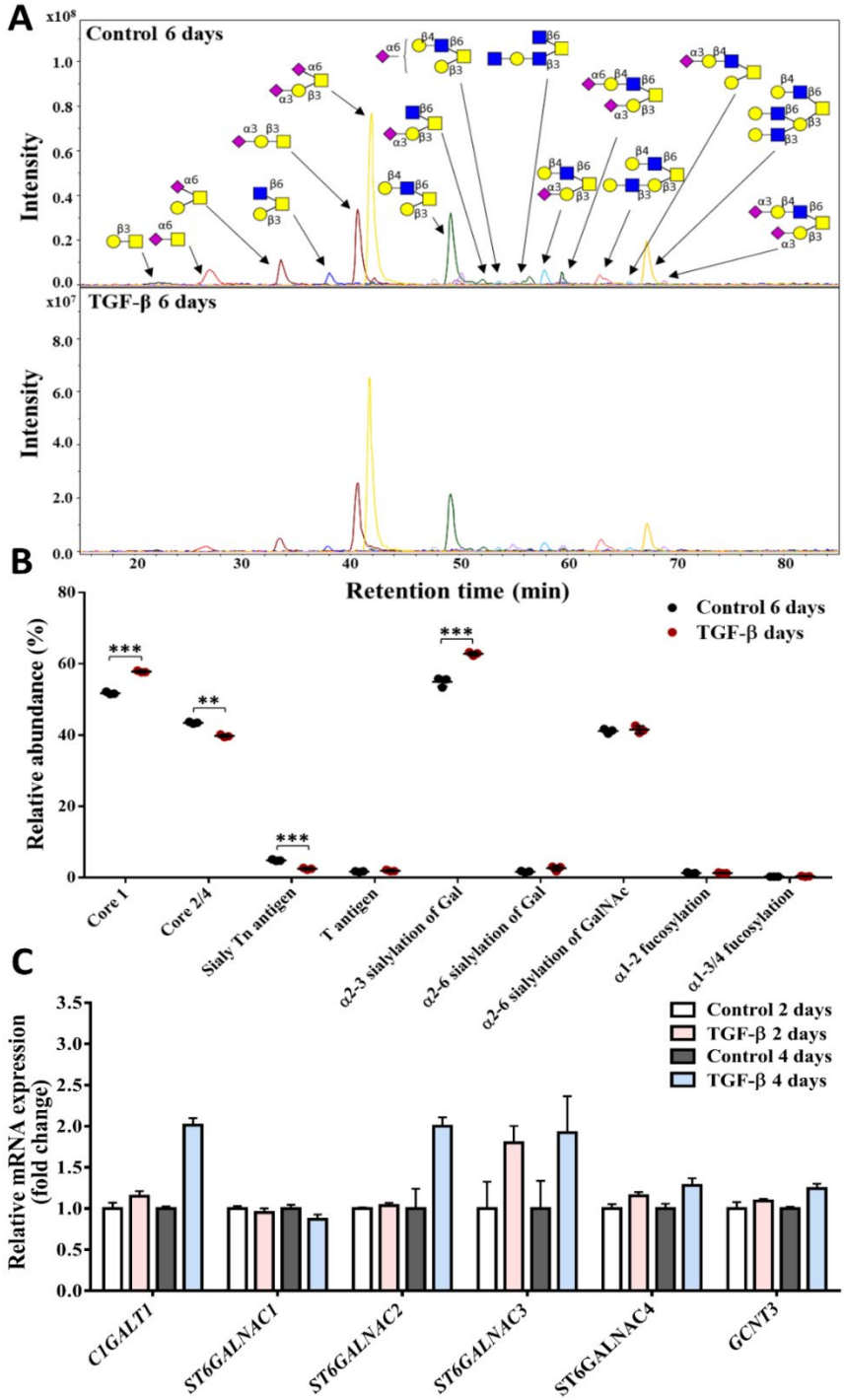

Figure 3. Differences of *O*-glycosylation in PaTu-S cell line without or with TGF-β

treatment. (A) Combined EICs of *O*-glycans were derived from PaTu-S cells treated with vehicle control or TGF-β for 6 days; both conditions show similar *O*-glycan profile. **(B)** Relative abundance of structural *O*-glycan classes in PaTu-S cells treated with vehicle control or TGF-β for 6 days. **(C)** qRT-PCR analysis of *O*-glycosylation-associated gene expression levels in PaTu-S cells treated with vehicle control or TGF-β for 2 days or 4 days. GAPDH was used for normalization to get the relative mRNA expression, and then gene expression levels in the control groups (2 days and 4 days) were used for further normalize the genes in TGF-β-treated groups (2 days and 4 days) to get fold changes data. Representative results are shown of three independent experiments, or the data is expressed as the mean ± s.d. (n=3). *P ⩽ 0.05, **P ⩽ 0.01, ***P ⩽ 0.001. Fresh medium containing TGF-β (2.5 ng/mL) or vehicle control was added every 2 days in all experiments.

with the elevated levels of *ST3GALs* (Figure 2C, S2B), and in parallel to the sialylation differences of the *N*-glycome (Figure 2B). In contrast, α2,6 sialylation of galactose, α2,6 sialylation of GalNAc, α1,2 fucosylation of galactose or α1,3/4 fucosylation was unaffected (Figure 3B). Interestingly, we detected no difference of α2,6 sialylation of GalNAc between PaTu-S cells with and without TGF-β stimulation (Figure 3B), despite the upregulation of α2,6 sialyltransferase associated genes *ST6GALNACs (2, 3,* and *4)* (Figure 3C, S3B). For a complete overview of the glycan quantification data and glycosylation-associated gene expression levels, see Figure S3.

Neo-expression of globosides in GSL-glycomics of PaTu-S cells following TGF-β-treatment

Next, GSL-glycans were analyzed after enzymatic release of the glycan head group using EGCase I from purified GSLs derived from PaTu-S cells. GSL-Glycan profiles stayed largely unchanged upon TGF-β treatment except for the globoside fraction, which appeared to be specifically induced by the treatment, albeit with overall low expression levels compared to the other GSL classes (Figure 4A, 4B, Figure S4). Importantly, globosides including Gb3 and Gb4 were specifically present in PaTu-S cells after TGF-β treatment, as there was no globoside detected in the untreated sample (Figure 4B). Consistent with the glycomic data, upon TGF-β treatment, gene transcript data of day 2 also showed a 12-fold increased expression of *A4GALT*, which is the key gene for the biosynthesis of globosides (Figure 4C, S4B). Although the expression

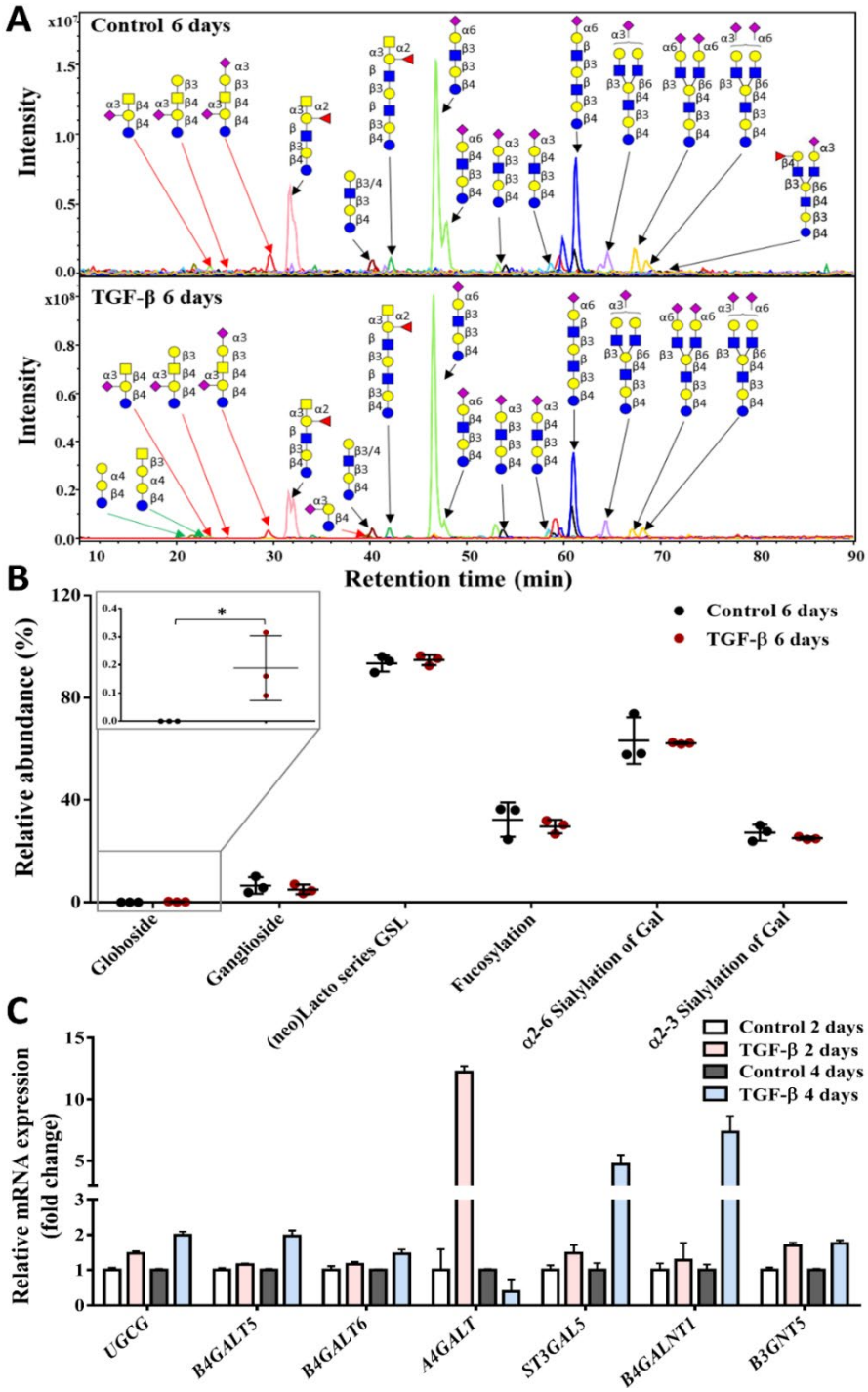

Figure 4. Differences of glycosphingolipid (GSL)-glycans in PaTu-S cell line without

or with TGF-β treatment. (A) Combined EICs of GSL-glycans were derived from PaTu-S cells treated with vehicle control or TGF-β for 6 days. Green arrow: globosides, red arrow: gangliosides, black arrow: (neo)lacto-series GSLs. **(B)** Relative abundance of structural GSL-glycan in PaTu-S cells treated with vehicle control or TGF-β for 6 days. **(C)** qRT-PCR analysis of glycosphingolipid-associated gene expression levels in PaTu-S cells treated with vehicle control or TGF-β for 2 days or 4 days. GAPDH was used for normalization to get the relative mRNA expression, and then gene expression levels in the control groups (2 days and 4 days) were used for further normalize the genes in TGF-β-treated groups (2 days and 4 days) to get fold changes data. Representative results are shown of three independent experiments, or the data is expressed as the mean ± s.d. (n=3). *P ⩽ 0.05, **P ⩽ 0.01, ***P ⩽ 0.001. Fresh medium containing TGF-β (2.5 ng/mL) or vehicle control was added every 2 days in all experiments.

levels of multiple GSL-associated genes were promoted after TGF-β stimulation for 4 days (Figure 4C, S4B), there was no significant difference in gangliosides, (neo)lacto series glycosphingolipids, α2,6 sialic acid on galactose, α2,3 sialic acid on galactose, and fucosylation (Figure 4B). For a complete overview of the GSLs quantification data and GSL-associated gene expression levels, see Figure S4.

SOX4 is required for TGF-β-induced promotion of *N*-glycosylation.

SOX4 is a key transcriptional target of the TGF-β signaling pathway [28] in various cell types, including breast epithelial cells [78], glioma cells [79], and pancreatic cancers [30]. Importantly, SOX4 is induced by TGF-β in a SMAD4-independent manner and promotes tumorigenesis in SMAD4-null pancreatic ductal adenocarcinoma cells [30]. Similarly, we found that SOX4 mRNA (Figure 5A) and protein expression levels (Figure 5B) were upregulated in PaTu-S cells upon TGF-β stimulation for 2 days and 4 days. To investigate the role of SOX4 in regulating the TGF-β-induced changes in glycan profile, we depleted the SOX4 using two shRNAs in PaTu-S cells. Expression of SOX4 was significantly decreased both at the mRNA (Figure 5C) and protein level (Figure 5D) in SOX4 knockdown cells. Moreover, SOX4 induction by TGF-β was eliminated by the shRNA-mediated SOX4 depletion (Figure S5A). The SOX4 knockdown efficiency was further validated by the monitoring (downregulated) expression of the established SOX4 target gene, *Nestin* (Figure S5B, C) [30]. TGF-β-induced upregulation of *N*-glycosylation-associated genes, including *MGAT4A* and *MGAT4B,* were attenuated by

SOX4 depletion (Figure 5E, Figure S5D). Accordingly, the relative abundance of complex and specifically triantennary *N*-glycans did not increase any more with SOX4 depletion even after TGF-β treatment for 6 days (Figure 5F, S5E). The same attenuation was observed in sialylation, as a result of the lower expression of *ST3GAL2, 3, 4,* and *ST6GAL1* in the TGF-β-treated SOX4 knockdown cells compared to the empty vector group in the presence of TGF-β (Figure 5E, Figure S5D). The TGF-β-induced increase in core fucosylation was downregulated by SOX4 knockdown in PaTu-S cells, as well as the downregulation of *FUT8* expression (Figure 5E, F, S5D, E). To further validate our results obtained by shRNA-mediated SOX4 depletion in TGF-β-induced upregulation of *N*-glycosylation, we used an alternative method to knockdown SOX4 expression, i.e., by CRISPR interference (CRISPRi). QPCR and Western blot assays revealed the decreased expression of SOX4 at the gene and protein level, respectively, in guide-RNA-mediated SOX4 knockdown cells (Figure S6A, B). Consistently, TGF-β-induced increases in complex structures, as well as the gene expression levels including *MGAT4A, MGAT4B*, were attenuated by CRISPRi-mediated SOX4 depletion (Figure S6C, D). Correspondingly, the upregulation of core fucosylation with TGF-β stimulation was inhibited, resulting from the downregulated expression level of the gene *FUT8* by SOX4 knock down (Figure S6C, D). SOX4 depletion also significantly decreased the relative abundance of sialylation and expression levels of associated genes, i.e., *ST3GAL2*, *ST3GAL4,* and *ST6GAL1* (Figure S6C, D). These results indicated that SOX4 is a critical mediator for TGF-β signaling in the PaTu-S cell line. SOX4 plays a key role in the TGF-β-mediated glycosylation responses, in particular in increasing the levels of sialylation, branching and core fucosylation within the *N*-glycan pool.

Additionally, we expanded our study to other SMAD4-deficient pancreatic adenocarcinoma cell lines such as CFPAC-1 and BxPC-3 cells [80]. Consistent with the results obtained with PaTu-S cells, we observed that TGF-β induced pSmad2 levels in CFPAC-1 and BxPC-3 cells (Figure S7A). This response was more efficient in BxPC-3 than CFPAC-1 cells, and therefore BxPC-3 cells were chosen for further study. Upon treatment of BxPC-3 cells with TGF-β, typical TGF-β target genes such as *CCN2,*

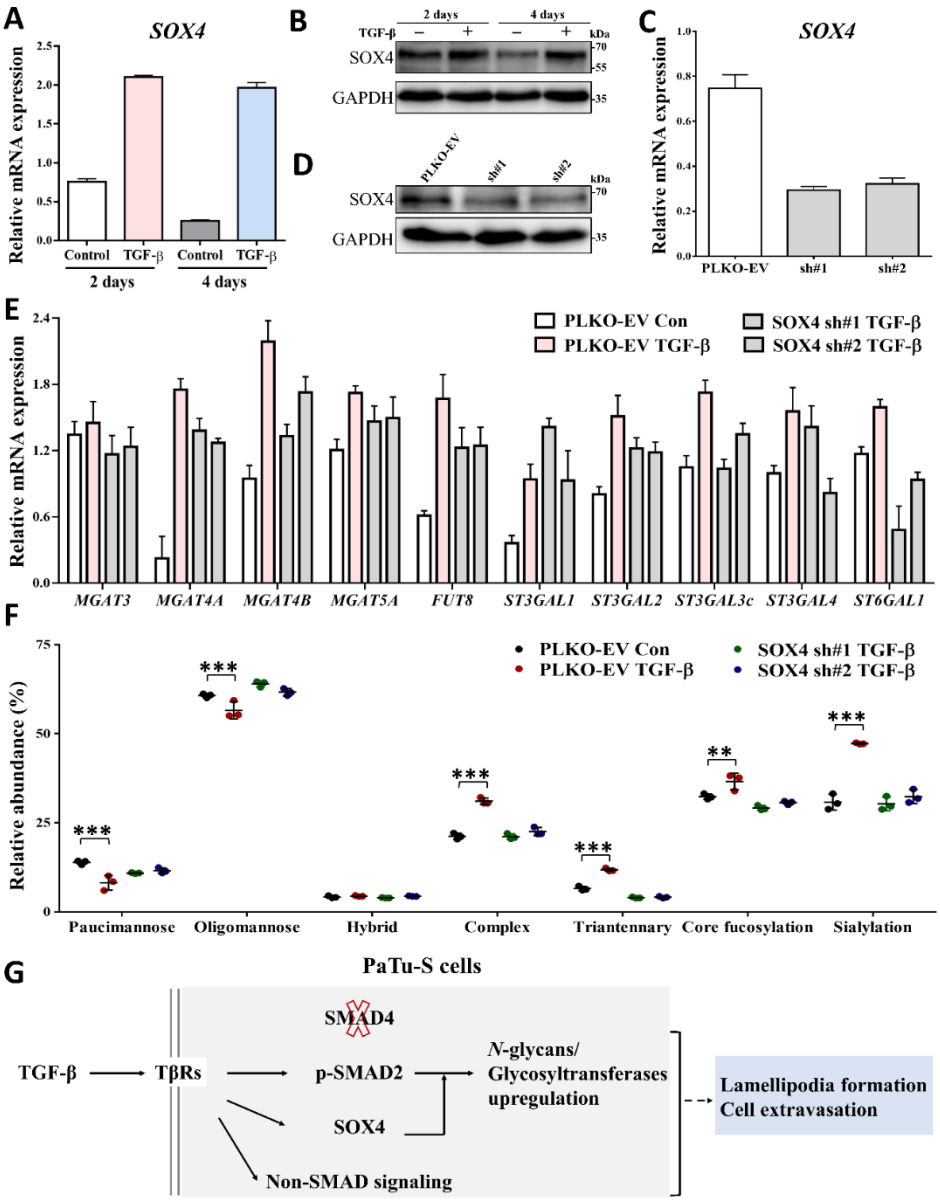

Figure 5. SOX4, a TGF-β target gene/protein, is needed for TGF-β-induced upregulation of *N*-glycans in PaTu-S cells. (A) qRT-PCR analysis of the SOX4 in PaTu-S cells treated with vehicle control or TGF-β for 2 days and 4 days. GAPDH mRNA levels were used for normalization. **(B)** Immunoblotting of cell lysates for SOX4 and GAPDH (as loading control); cells were treated with vehicle control or TGF-β for 2 days and 4 days. The molecular weight markers are indicated on the right. **(C)** PaTu-S cells were stably infected with two SOX4 shRNAs (sh#1 and sh#2) or empty vector shRNA (PLKO-EV). qRT-PCR analysis was used for the expression of SOX4 mRNA.

(D) Western blot analysis of SOX4 expression in PaTu-S cells infected with PLKO-EV, SOX4 sh#1 and SOX4 sh#2. The molecular weight markers are indicated on the right. and GAPDH, loading control. **(E)** qRT-PCR analysis of *N*-glycosylation-associated transcripts in PaTu-S cells with PLKO-EV, SOX4 sh#1 and SOX4 sh#2 after treatment with vehicle control (Con) or TGF-β for 2 days. **(F)** Relative abundance of structural *N*-glycan classes derived from PaTu-S cells with PLKO-EV, SOX4 sh#1 and SOX4 sh#2 were treated with vehicle control or TGF-β for 6 days on PGC nano-LC-ESI-MS/MS in negative ion mode. **(G)** Summary diagram showing the essential role of SOX4 in TGF-β-induced upregulation of N-glycans and associated glycosyltransferases in SMAD4 deficient PaTu-S cells. The role, if any of, changes in glycosylation in TGF-β-induced biological responses, such as the F-actin formation and cell extravasation, requires further studies. Fresh medium containing TGF-β (2.5 ng/mL) or vehicle control was added every 2 days in all experiments. Representative results are shown of three independent experiments, or the data is expressed as the mean ± s.d. (n=3).

SERPINE1, and *SMAD7* were found to be upregulated (Figure S7B). Moreover, TGF-β induced the expression of mesenchymal markers including *CDH2*, *SNAI1,* and *VIM* at the mRNA level, but only the protein expression of N-cadherin was increased by TGF-β in BxPC-3 cells (Figure S7C, D). The results obtained with BxPC3 are comparable to the results we obtained using PaTu-S cells. However, the *N*-glycosylation-associated genes, including *MGAT4A, MGAT4B, MGAT5A, FUT8, ST6GAL1,* and *FUT1*, were only slightly induced by TGF-β treatment for 2 days or 4 days (Figure S7E). Thus, the glycomic response to TGF-β in BxPC-3 cells is weaker than that obtained in PaTu-S cells. To investigate the role of SOX4 in BxPC-3 cells, we depleted the SOX4 with two independent shRNAs in BxPC-3 cells and validated the SOX4 knockdown by qRT-PCR and Western blotting (Figure S8A, B). The TGF-β-induced upregulation of *N*-glycosylation-associated genes *MGAT5A* and *ST6GAL1* was inhibited by SOX4 knockdown (Figure S8C). Thus, SOX4 plays a role in TGF-β-mediated increase of *N*-glycan-associated genes in multiple SMAD4-deficient PDAC lines.

Discussion

Here, we provide a comprehensive analysis of TGF-β-induced *N*-glycan, *O*-glycan, and GSL-glycan patterns in PaTu-S pancreatic adenocarcinoma cells. Our study demonstrated the significant upregulation of branching,

sialylation, and core fucosylation of *N*-glycans in TGF-β-treated PaTu-S cells in a SMAD4-independent manner. These *N*-glycosylation changes were found to be largely mirrored by transcriptomic changes of the underlying glycotransferase-associated genes. Indeed, several studies have shown that TGF-β-mediated *N*-glycosylation changes are involved in the TGF-β-SMAD4 signaling pathway but rarely in SMAD4-independent pathways. For example, *ST6GAL1* and its enzymatic products including α2,6-sialylation are significantly increased during TGF-β-SMADs-induced EMT in the mouse epithelial GE11 (SMAD4 active) cell line, which further regulates the cell migration and invasion [81]. In our study, the similar upregulation of *ST6GAL1* gene expression level and sialylation was observed in the SMAD4-deficient PaTu-S cell line. Thus, further functional studies are required to investigate the role of these specific glycosylation changes during TGF-β stimulation in SMAD4-deficient PDAC. In addition, the significant upregulation of *O*-glycosylation by TGF-β treatment, which is independent of SMAD4, in the PaTu-S cell line only happened in several types of glycans such as α2,3 sialylation of galactose and core 1 structures. Importantly, the sialylated Tn antigen was notably decreased by TGF-β stimulation in Patu-S cells, which is carried by various glycoproteins and is associated with cancer progression, invasion and metastasis in some published studies [82, 83]. In line with this TGF-β-induced downregulation, we have also observed the loss of sialylated Tn antigen in the mesenchymal-like Pa-Tu-8988T (PaTu-T) cells [84], which was derived from the same patient as the PaTu-S cell line. These results together indicate a potential role of sialylated Tn antigen in TGF-β signaling and response in the PaTu-S cell line.

GSLs were shown to be involved in the TGF-β-induced EMT process in normal murine mammary gland NMuMG [85] and human mammary carcinoma MCF7 cells [86], both of which express SMAD4. The promotion or inhibition of TGF-β-induced EMT and cell migration and metastasis by certain GSL, including gangliosides GM2, Gg4, GM3 and GD2, have been studied in the SMAD4-dependent TGF-β response. In the SMAD4-deficient PaTu-S cell line, the only significant differences were the specific expression of globosides Gb3 and Gb4 despite the

upregulation of GSLs-associated genes upon TGF-β stimulation. This phenomenon suggests that increased gene expression may not result in an increased level of protein expression/activity [87, 88]. The neo-expression of globosides following TGF-β treatment is an interesting observation since Gb3 has been reported to be associated with tumor invasion and metastasis in many cancers, including lung cancer [89], colon cancer [90, 91], breast cancer [92], gastric adenocarcinomas [93], and pancreatic cancer [94]. In addition, A4GALT, a key enzyme for globoside biosynthesis, can induce EMT and mediate cell–cell adhesion in ovarian cancer cells [88]. In our previous study, globoside Gb3 and Gb4 were specifically expressed in the mesenchymal-like PaTu-T cells compared to epithelial PaTu-S cells [84]. Again, these findings suggest that the globosides may contribute to the invasion and metastasis in PDAC. In the future, it will be of interest to investigate the role of sialylated Tn antigen and globosides, especially Gb3, in TGF-β-mediated PDAC progression.

Importantly, we showed that *SOX4*, a TGF-β transcriptional target gene, is required for TGF-β-induced increases in *N*-glycosylation. Knockdown of SOX4 in PaTu-S cells resulted in the attenuation of TGF-β-mediated increases in branching structures, sialylation, and core fucosylation. Since SOX4 was shown to promote tumorigenesis in PDAC cells independent of SMAD4 expression [30], it will be interesting to investigate the relationship between TGF-β-SOX4-mediated glycosylation changes and tumorigenesis in SMAD4 deficient cells. A recent study demonstrated that the integrin αvβ6-TGF-β-SOX4 pathway regulates multiple signaling events relevant for T cell-mediated tumor immunity in triple-negative breast cancer cells [95]. Our previous study of glycosylation in PaTu-S cells revealed that these cells bind to dendritic cells (DCs) via galectins and other lectins, which may have effects on the immune response [84]. Thus, the TGF-β-SOX4 signaling pathway-induced upregulation of *N*-glycosylation especially branching, sialylation and core fucosylation might impact on immune responses in PaTu-S cells. We extended our results on PaTu-S cells to include another SMAD4-deficient PDAC line, i.e., BxPC3 cells. We found a relatively weak glycomic response to TGF-β, and that SOX4 depletion decreased the TGF-β-induced increase in *N*-glycan-associated genes in BxPC-3 cells (Figure S8C).

In our study, loss of SMAD4 had no effect on the phosphorylation of the upstream protein, SMAD2, upon TGF-β stimulation in multiple SMAD4 deficient PDAC lines. Interestingly, we found that TGF-β can still significantly promote the mRNA expression of TGF-β target genes, including *CCN2, SERPINE1, PTHLH,* and *SMAD7* in SMAD4 deficient PaTu-S and BxPC3 cell lines. This upregulation of TGF-β target genes indicates that some genes do not require SMAD4 for their regulation. Large-scale microarray analysis, which used a tetracycline-inducible small interfering RNA (siRNA) of SMAD4 [96], identified two populations of TGF-β target genes based upon their (in)dependency on SMAD4 in human immortalized keratinocytes (HaCaT) cells [72]. Indeed, many TGF-β target genes such as *PTHLH* and *SMAD7* were not affected by SMAD4 depletion. Although the *SERPINE1* gene was classified in the category of SMAD4 dependent genes in this study [72], the authors also emphasized that this gene still displayed a residual induction with TGF-β stimulation after SMAD4 silencing [72]. The previous study also demonstrated that the gene expression level of *CCN2* (encoding the protein CTGF) can be induced by the combination of direct SMAD phosphorylation and indirect JAK/STAT3 activation in activated hepatic stellate cells (HSCs) [97]. These reports suggest that TGF-β target genes can be regulated by both SMAD4-dependent and SMAD4-independent pathways. Our data regarding the TGF-β-induced changes in gene expression in the SMAD4 deficient PaTu-S and BxPC-3 cell lines provide further support for this notion. Moreover, we found that SOX4 knockdown had no effect on the TGF-β-mediated increase of target genes *CCN2, SERPINE1, PTHLH,* and *SMAD7* in PaTu-S cells (Figure S9). This indicates that expression of these TGF-β-induced target genes is regulated in a SMAD4- and SOX4-independent manner.

We investigated the changes in expression of EMT markers upon TGF-β treatment both at the gene and protein level in PaTu-S and BxPC-3 cells. Mesenchymal markers such as N-cadherin (encoded by the *CDH2* gene), SLUG (encoded by the *SNAL2* gene), and vimentin (encoded by the *VIM* gene) are induced by TGF-β treatment for 2 days at the mRNA level. At the protein level, N-cadherin (but not SLUG and vimentin (data not shown) were upregulated in response to TGF-β stimulation for 2 days and 4 days

in PaTu-S and BxPC-3 cells. In addition, expression and localization of the epithelial marker E-cadherin were barely affected by TGF-β after 2 days and 4 days of treatment. Our results indicate that these two SMAD4 deficient cell lines, including the PaTu-S and BxPC-3 cell lines, do not undergo a complete TGF-β-induced EMT. Similar results were also shown in the previous study [30] that SMAD4-mutant cells retained E-cadherin expression after TGF-β treatment for 36 h. In addition, we found that TGF-β promotes lamellipodia formation in PaTu-S cells, using immunofluorescence staining of the actin cytoskeleton and extravasation using a zebrafish xenograft model. Indeed, TGF-β leads to rearrangements of the actin filament network via canonical and non-canonical TGF-β signaling [98-100]. In human prostate carcinoma cells, TGF-β treatment induced a rapid formation of lamellipodia through the SMAD-independent signaling pathway, which requires the activation of the Rho-family GTPases including CDC42 and RHOA [101]. Thus, the investigation of the role of altered glycosylation in TGF-β-induced lamellipodia formation in PaTu-S cells may offer clues as to how TGF-β mediates invasion in the zebrafish model and also provides a basis for further studies.

Experimental procedures

Materials and chemicals

Ammonium acetate, ammonium bicarbonate, cation exchange resin beads (AG50W-X8), trifluoroacetic acid (TFA), potassium hydroxide, and sodium borohydride were obtained from Sigma-Aldrich (Steinheim, Germany). 8 M guanidine hydrochloride (GuHCl) was obtained from Thermo Fisher Scientific (Waltham, MA). TGF-β3 was generously provided by Dr. A. Hinck (University of Pittsburg, PA). Dithiothreitol (DTT), HPLC SupraGradient acetonitrile (ACN) was obtained from Biosolve (Valkenswaard, The Netherlands), and other reagents and solvents such as chloroform, methanol, ethanol, 2-propanol, and glacial acetic acid were from Merck (Darmstadt, Germany). MultiScreen® HTS 96 multi-well plates (pore size 0.45 μm) with high protein-binding membrane (hydrophobic Immobilon-P PVDF membrane) were purchased

from Millipore (Amsterdam, The Netherlands), conical 96-well Nunc plates from Thermo Fisher. The 50 mg TC18-reverse phase (RP)-cartridges were from Waters (Breda, The Netherlands). Peptide N-glycosidase F (PNGase F, lyophilized, glycerol-free) was purchased from Roche Diagnostics (Mannheim, Germany). SB431542 was from Tocris Biosciences (1614, Abingdon, United Kingdom), Alexa Fluor 488 Phalloidin was purchased from Thermo Fisher (A12379). Endoglycoceramidase I (EGCase I, recombinant clone derived from *Rhodococcus triatomea* and expressed in *Escherichia coli*) and 10x EGCase I buffer (500 mM HEPES, 1M NaCl, 20 mM DTT and 0.1% Brij 35, pH 5.2) were purchased from New England BioLabs Inc. (Ipswich, MA). Ultrapure water was used for all preparations and washes, generated from a Q-Gard 2 system (Millipore, Amsterdam, The Netherlands).

Primers and antibodies

The DNA sequences of human forward and reverse primers that were used to detect the expression of specific genes are listed in Table S4. The antibodies that were used for immunoblotting (IB) and immunofluorescence (IF): phosphor-SMAD2 1:1000 (IB: 3108, Cell signaling), GAPDH 1:1000 (IB: MAB374, Millipore), E-cadherin 1:1000 (IB, IF: 610181, BD Biosciences), N-cadherin 1:1000 (IB: 610920, BD Biosciences), SLUG 1:1000 (IB: 9585, Cell Signaling), SOX4 1:1000 (IB: Diagenode, C15310129), Vinculin (IB: V9131, Sigma), Alexa Fluor 555 secondary antibody 1:500 (IF: A-21422, Thermo Fisher).

Cell culture

PaTu-8988S (PaTu-S) cell line was obtained from DSMZ culture bank (Braunschweig, Germany) [102]. Human embryonic kidney (HEK) 293T, A549-vimentin (VIM)- red fluorescent protein (RFP), pancreatic adenocarcinoma BxPC-3, CFPAC-1 cell lines were originally purchased from American Type Culture Collection (ATCC). PaTu-S, HEK293T, A549-VIM-RFP, and CFPAC-1 cells were cultured in Dulbecco's modified Eagle medium (DMEM) with 10% fetal bovine serum (FBS) and 100U/mL penicillin-streptomycin. BxPC-3 cells were maintained in RPMI-1640, supplemented with 10% FBS and 100U/mL penicillin-streptomycin. These cell lines were frequently tested for the absence of

mycoplasma contamination and authenticated by short tandem repeat (STR) profiling. For all the experiments mentioned in this study, the PaTu-S cells were always starved in DMEM with 0.5% serum for 6 h before adding ligands. The concentration of TGF-β was applied as 2.5 ng/mL, and the same volume of ligand buffer (4 mM HCl, 0.1% BSA) was used as a vehicle control.

Plasmid construction, single guide (sg) RNA design, and shRNA selection

The human SOX4 sgRNAs were designed using the online tool CHOPCHOP (https://chopchop.cbu.uib.no/), and two independent sgRNAs with the lowest off-activity were chosen. The two complementary sgRNAs contain *Bve*I cut sites, and their sequences are listed in Table S4. The pLKO.1-puro.U6.sgRNA *Bve*I stuffer lentiviral vector was used as a backbone to generate AA19 pLKO.1-SOX4-sgRNA plasmid and obtained from Addgene. The dCas9-KRAB-T2A-puro lentiviral plasmid was from Addgene (#99372).

SOX4 short hairpin (sh)RNAs for lentiviral transduction were obtained from Sigma (MISSION shRNA library). We tested six SOX4 shRNAs; the two most effective shRNAs for PaTu-S cells were used for further experiments. These were sh#1-SOX4 (TRCN0000018217, 5'-GAAGAAGGTGAAGCGCGTCTA-3') with PLKO.1-puro vector and sh#2-SOX4 (TRCN0000274207, 5'-GAAGAAGGTGAAGCGCGTC TA-3') with a vector of TRC2-PLKO-puro. These two shRNAs have almost identical target sequences, but the sh#2-SOX4 contains a woodchuck hepatitis post-transcriptional regulatory element (WPRE) in its backbone vector. For the SOX4 knockdown of BxPC-3 cells, we used two independent shRNAs, including sh#2-SOX4 and sh#12-SOX4 (TRCN0000018213, 5'-CCTTTCTACTTGTCGCTAAAT-3'). The PLKO.1-puro empty vector (SHC001, Sigma) was used as a negative control (it does not contain an shRNA insert).

Lentiviral transduction and generation of stable cell lines

Lentiviruses were produced by transfecting HEK293T cells with shRNA plasmids, PLKO empty vector, PLV-mCherry, AA19 pLKO.1-SOX4-sgRNA plasmids or dCas9-KRAB-T2A-puro lentiviral plasmid, and three

packaging plasmids that are pCMV-G protein of the vesicular stomatitis virus (VSVG), pMDLg-RRE (gag-pol) and pRSV-REV as described [103]. The viral supernatants were harvested at 48 hours (h) post-transfection and filtered through a 0.45 μm polyethersulfone (PES) filter. Viruses were either directly used for infection or stored at -80 °C as soon as possible to avoid loss of titer.

To generate stable SOX4 knockdown cell lines, we first prepared a 1:1 dilution of the lentivirus in DMEM complemented with 5 ng/mL of Polybrene (Sigma). Thereafter, PaTu-S cells or BxPC-3 cells were infected with the lentiviral dilution at a low cell density (30%). After infection for 48 h, cells were selected with 2 μg/mL of puromycin for one week in order to generate the SOX4-depleted cells.

The PaTu-S mCherry cells were infected with PLV-mCherry lentivirus, and a single colony that highly expresses mCherry was isolated by FACS sorting for high mCherry expression. Thereafter, high mCherry sorted (PaTu-S mCherry) cells were cultured and expanded.

Statistical analysis

Statistical analyses were performed with a Student's unpaired t-test using Prism 8 software (GraphPad La Jolla, CA). The numerical data from triplicates, PGC nano-LC-ESI-MS/MS and the Zebrafish assay are expressed as the mean ± s.d. P-value is indicated by asterisks in the figures, $*P \leq 0.05$, $**P \leq 0.01$, $***P \leq 0.001$. $P \leq 0.05$ was considered statistically significant.

Acknowledgments

We acknowledge the support of the Chinese Scholarship Council (CSC) to Jing Zhang, Cancer Genomics Centre Netherlands (CGC. NL) to Peter ten Dijke, and Austrian Science Fund (FWF, W1213) to Constantin Blöchl. We thank Irma van Die and Ana I. Belo for the contribution of the PaTu-S cell line and fruitful discussions. We thank David Baker for the valuable discussion and proofreading of the paper.

Data availability

The raw mass spectrometric data files that support the findings of this study are available in GlycoPOST in mzXML format, with the identifier GPST000218, accessible via the following link https://glycopost.glycosmos.org/entry/GPST000218.

Supplementary Information

Supplementary methods, Supplementary Figure S1-S9 and Tables S1-S4 are available upon request using the following link:

https://www.jbc.org/article/S0021-9258(22)00157-0/fulltext

References

1. Siegel, R.L., K.D. Miller, and A. Jemal, Cancer statistics, 2019. CA Cancer J Clin, 2019. 69(1): p. 7-34.
2. Vincent, A., et al., Pancreatic cancer. Lancet, 2011. 378(9791): p. 607-20.
3. Jones, S., et al., Core signaling pathways in human pancreatic cancers revealed by global genomic analyses. Science, 2008. 321(5897): p. 1801-6.
4. Pan, S., T.A. Brentnall, and R. Chen, Proteome alterations in pancreatic ductal adenocarcinoma. Cancer Lett, 2020. 469: p. 429-436.
5. Fischer, C.G. and L.D. Wood, From somatic mutation to early detection: insights from molecular characterization of pancreatic cancer precursor lesions. J Pathol, 2018. 246(4): p. 395-404.
6. Distler, M., et al., Precursor lesions for sporadic pancreatic cancer: PanIN, IPMN, and MCN. Biomed Res Int, 2014. 2014: p. 474905.
7. Hruban, R.H., A. Maitra, and M. Goggins, Update on pancreatic intraepithelial neoplasia. Int J Clin Exp Pathol, 2008. 1(4): p. 306-16.
8. Murphy, S.J., et al., Genetic alterations associated with progression from pancreatic intraepithelial neoplasia to invasive pancreatic tumor. Gastroenterology, 2013. 145(5): p. 1098-1109 e1.
9. Eser, S., et al., Selective requirement of PI3K/PDK1 signaling for Kras oncogene-driven pancreatic cell plasticity and cancer. Cancer Cell, 2013. 23(3): p. 406-20.
10. Ardito, C.M., et al., EGF receptor is required for KRAS-induced pancreatic tumorigenesis. Cancer Cell, 2012. 22(3): p. 304-17.

11. Perkhofer, L., et al., DNA damage repair as a target in pancreatic cancer: state-of-the-art and future perspectives. Gut, 2020.
12. Itakura, J., et al., Enhanced expression of vascular endothelial growth factor in human pancreatic cancer correlates with local disease progression. Clin Cancer Res, 1997. 3(8): p. 1309-16.
13. Niedergethmann, M., et al., High expression of vascular endothelial growth factor predicts early recurrence and poor prognosis after curative resection for ductal adenocarcinoma of the pancreas. Pancreas, 2002. 25(2): p. 122-9.
14. Chen, R., et al., Pancreatic cancer proteome: the proteins that underlie invasion, metastasis, and immunologic escape. Gastroenterology, 2005. 129(4): p. 1187-97.
15. Yachida, S., et al., Distant metastasis occurs late during the genetic evolution of pancreatic cancer. Nature, 2010. 467(7319): p. 1114-7.
16. Qian, Y., et al., Molecular alterations and targeted therapy in pancreatic ductal adenocarcinoma. J Hematol Oncol, 2020. 13(1): p. 130.
17. Kabacaoglu, D., et al., Immune Checkpoint Inhibition for Pancreatic Ductal Adenocarcinoma: Current Limitations and Future Options. Front Immunol, 2018. 9: p. 1878.
18. Colak, S. and P. Ten Dijke, Targeting TGF-β Signaling in Cancer. Trends Cancer, 2017. 3(1): p. 56-71.
19. Batlle, E. and J. Massague, Transforming Growth Factor-β Signaling in Immunity and Cancer. Immunity, 2019. 50(4): p. 924-940.
20. Massague, J., How cells read TGF-β signals. Nat Rev Mol Cell Biol, 2000. 1(3): p. 169-78.
21. Massague, J., TGFβ signalling in context. Nat Rev Mol Cell Biol, 2012. 13(10): p. 616-30.
22. Heldin, C.H., K. Miyazono, and P. ten Dijke, TGF-β signalling from cell membrane to nucleus through SMAD proteins. Nature, 1997. 390(6659): p. 465-71.
23. Budi, E.H., D. Duan, and R. Derynck, Transforming Growth Factor-β Receptors and Smads: Regulatory Complexity and Functional Versatility. Trends Cell Biol, 2017. 27(9): p. 658-672.
24. Lagna, G., et al., Partnership between DPC4 and SMAD proteins in TGF-β signalling pathways. Nature, 1996. 383(6603): p. 832-6.
25. Zhang, Y., et al., Receptor-associated Mad homologues synergize as effectors of the TGF-β response. Nature, 1996. 383(6596): p. 168-72.
26. Schuster, N. and K. Krieglstein, Mechanisms of TGF-β-mediated apoptosis. Cell Tissue Res, 2002. 307(1): p. 1-14.
27. Dardare, J., et al., SMAD4 and the TGFβ Pathway in Patients with Pancreatic Ductal Adenocarcinoma. Int J Mol Sci, 2020. 21(10).

28. Vervoort, S.J., et al., SOX4 can redirect TGF-β-mediated SMAD3-transcriptional output in a context-dependent manner to promote tumorigenesis. Nucleic Acids Res, 2018. 46(18): p. 9578-9590.
29. Isogaya, K., et al., A Smad3 and TTF-1/NKX2-1 complex regulates Smad4-independent gene expression. Cell Res, 2014. 24(8): p. 994-1008.
30. David, C.J., et al., TGF-β Tumor Suppression through a Lethal EMT. Cell, 2016. 164(5): p. 1015-30.
31. Zhang, J., et al., SOX4 induces epithelial-mesenchymal transition and contributes to breast cancer progression. Cancer Res, 2012. 72(17): p. 4597-608.
32. Zhang, Y.E., Non-Smad Signaling Pathways of the TGF-β Family. Cold Spring Harb Perspect Biol, 2017. 9(2).
33. Lee, M.K., et al., TGF-β activates Erk MAP kinase signalling through direct phosphorylation of ShcA. EMBO J, 2007. 26(17): p. 3957-67.
34. Arsura, M., et al., Transient activation of NF-kappaB through a TAK1/IKK kinase pathway by TGF-β1 inhibits AP-1/SMAD signaling and apoptosis: implications in liver tumor formation. Oncogene, 2003. 22(3): p. 412-25.
35. Descargues, P., et al., IKKalpha is a critical coregulator of a Smad4-independent TGFβ-Smad2/3 signaling pathway that controls keratinocyte differentiation. Proc Natl Acad Sci U S A, 2008. 105(7): p. 2487-92.
36. Moustakas, A. and C.H. Heldin, Non-Smad TGF-β signals. J Cell Sci, 2005. 118(Pt 16): p. 3573-84.
37. Yamashita, M., et al., TRAF6 mediates Smad-independent activation of JNK and p38 by TGF-β. Mol Cell, 2008. 31(6): p. 918-24.
38. Zhang, L., et al., TRAF4 promotes TGF-β receptor signaling and drives breast cancer metastasis. Mol Cell, 2013. 51(5): p. 559-72.
39. Derynck, R. and R.A. Weinberg, EMT and Cancer: More Than Meets the Eye. Dev Cell, 2019. 49(3): p. 313-316.
40. Moustakas, A. and C.H. Heldin, Mechanisms of TGFβ-Induced Epithelial-Mesenchymal Transition. J Clin Med, 2016. 5(7).
41. Katsuno, Y., S. Lamouille, and R. Derynck, TGF-β signaling and epithelial-mesenchymal transition in cancer progression. Curr Opin Oncol, 2013. 25(1): p. 76-84.
42. Yang, J., et al., Guidelines and definitions for research on epithelial-mesenchymal transition. Nat Rev Mol Cell Biol, 2020. 21(6): p. 341-352.
43. Saxena, K., M.K. Jolly, and K. Balamurugan, Hypoxia, partial EMT and collective migration: Emerging culprits in metastasis. Transl Oncol, 2020. 13(11): p. 100845.
44. Pinho, S.S. and C.A. Reis, Glycosylation in cancer: mechanisms and clinical implications. Nat Rev Cancer, 2015. 15(9): p. 540-55.

45. Munkley, J., The glycosylation landscape of pancreatic cancer. Oncol Lett, 2019. 17(3): p. 2569-2575.
46. Zhang, J., et al., Role of glycosylation in TGF-β signaling and epithelial-to-mesenchymal transition in cancer. Protein Cell, 2021. 12(2): p. 89-106.
47. Yang, Y., J.D. Dignam, and L.E. Gentry, Role of carbohydrate structures in the binding of β1-latency-associated peptide to ligands. Biochemistry, 1997. 36(39): p. 11923-32.
48. Kim, Y.W., et al., TGF-β sensitivity is determined by N-linked glycosylation of the type II TGF-β receptor. Biochem J, 2012. 445(3): p. 403-11.
49. Li, X., et al., Role of Glycans in Cancer Cells Undergoing Epithelial-Mesenchymal Transition. Front Oncol, 2016. 6: p. 33.
50. Huang, C., et al., N-acetylglucosaminyltransferase V modulates radiosensitivity and migration of small cell lung cancer through epithelial-mesenchymal transition. FEBS J, 2015. 282(22): p. 4295-306.
51. Xu, Q., et al., Roles of N-acetylglucosaminyltransferase III in epithelial-to-mesenchymal transition induced by transforming growth factor β1 (TGF-β1) in epithelial cell lines. J Biol Chem, 2012. 287(20): p. 16563-74.
52. Wang, M., et al., Aberrant glycosylation and cancer biomarker discovery: a promising and thorny journey. Clin Chem Lab Med, 2019. 57(4): p. 407-416.
53. Yue, T., et al., The prevalence and nature of glycan alterations on specific proteins in pancreatic cancer patients revealed using antibody-lectin sandwich arrays. Mol Cell Proteomics, 2009. 8(7): p. 1697-707.
54. Zhao, J., et al., N-linked glycosylation profiling of pancreatic cancer serum using capillary liquid phase separation coupled with mass spectrometric analysis. J Proteome Res, 2007. 6(3): p. 1126-38.
55. Pan, S., et al., Quantitative glycoproteomics analysis reveals changes in N-glycosylation level associated with pancreatic ductal adenocarcinoma. J Proteome Res, 2014. 13(3): p. 1293-306.
56. Nigjeh, E.N., et al., Spectral library-based glycopeptide analysis-detection of circulating galectin-3 binding protein in pancreatic cancer. Proteomics Clin Appl, 2017. 11(9-10).
57. Taniuchi, K., et al., Overexpression of GalNAc-transferase GalNAc-T3 promotes pancreatic cancer cell growth. Oncogene, 2011. 30(49): p. 4843-54.
58. Janik, M.E., A. Litynska, and P. Vereecken, Cell migration-the role of integrin glycosylation. Biochim Biophys Acta, 2010. 1800(6): p. 545-55.
59. Leeming, D.J., et al., Post-translational modifications of the extracellular matrix are key events in cancer progression: opportunities for biochemical marker development. Biomarkers, 2011. 16(3): p. 193-205.

60. Malik, R., P.I. Lelkes, and E. Cukierman, Biomechanical and biochemical remodeling of stromal extracellular matrix in cancer. Trends Biotechnol, 2015. 33(4): p. 230-6.
61. Provenzano, P.P. and S.R. Hingorani, Hyaluronan, fluid pressure, and stromal resistance in pancreas cancer. Br J Cancer, 2013. 108(1): p. 1-8.
62. Zhang, Y., et al., Tumor markers CA19-9, CA242 and CEA in the diagnosis of pancreatic cancer: a meta-analysis. Int J Clin Exp Med, 2015. 8(7): p. 11683-91.
63. Engle, D.D., et al., The glycan CA19-9 promotes pancreatitis and pancreatic cancer in mice. Science, 2019. 364(6446): p. 1156-1162.
64. Reitz, D., et al., Combination of tumour markers CEA and CA19-9 improves the prognostic prediction in patients with pancreatic cancer. J Clin Pathol, 2015. 68(6): p. 427-33.
65. Nie, S., et al., Glycoprotein biomarker panel for pancreatic cancer discovered by quantitative proteomics analysis. J Proteome Res, 2014. 13(4): p. 1873-84.
66. Meyer, C., et al., Distinct role of endocytosis for Smad and non-Smad TGF-β signaling regulation in hepatocytes. J Hepatol, 2011. 55(2): p. 369-78.
67. Samarakoon, R., et al., Induction of renal fibrotic genes by TGF-β1 requires EGFR activation, p53 and reactive oxygen species. Cell Signal, 2013. 25(11): p. 2198-209.
68. Dennler, S., et al., Direct binding of Smad3 and Smad4 to critical TGF β-inducible elements in the promoter of human plasminogen activator inhibitor-type 1 gene. EMBO J, 1998. 17(11): p. 3091-100.
69. Samarakoon, R. and P.J. Higgins, Integration of non-SMAD and SMAD signaling in TGF-β1-induced plasminogen activator inhibitor type-1 gene expression in vascular smooth muscle cells. Thromb Haemost, 2008. 100(6): p. 976-83.
70. Kakonen, S.M., et al., Transforming growth factor-β stimulates parathyroid hormone-related protein and osteolytic metastases via Smad and mitogen-activated protein kinase signaling pathways. J Biol Chem, 2002. 277(27): p. 24571-8.
71. Brodin, G., et al., Efficient TGF-β induction of the Smad7 gene requires cooperation between AP-1, Sp1, and Smad proteins on the mouse Smad7 promoter. J Biol Chem, 2000. 275(37): p. 29023-30.
72. Levy, L. and C.S. Hill, Smad4 dependency defines two classes of transforming growth factor β (TGF-β) target genes and distinguishes TGF-β-induced epithelial-mesenchymal transition from its antiproliferative and migratory responses. Mol Cell Biol, 2005. 25(18): p. 8108-25.

73. Krause, M. and A. Gautreau, Steering cell migration: lamellipodium dynamics and the regulation of directional persistence. Nat Rev Mol Cell Biol, 2014. 15(9): p. 577-90.
74. Zhang, T., et al., Development of a 96-well plate sample preparation method for integrated N- and O-glycomics using porous graphitized carbon liquid chromatography-mass spectrometry. Mol Omics, 2020.
75. Anugraham, M., et al., A platform for the structural characterization of glycans enzymatically released from glycosphingolipids extracted from tissue and cells. Rapid Commun Mass Spectrom, 2015. 29(7): p. 545-61.
76. Jensen, P.H., et al., Structural analysis of N- and O-glycans released from glycoproteins. Nat Protoc, 2012. 7(7): p. 1299-310.
77. Holst, S., et al., Profiling of different pancreatic cancer cells used as models for metastatic behaviour shows large variation in their N-glycosylation. Sci Rep, 2017. 7(1): p. 16623.
78. Vervoort, S.J., et al., SOX4 mediates TGF-β-induced expression of mesenchymal markers during mammary cell epithelial to mesenchymal transition. PLoS One, 2013. 8(1): p. e53238.
79. Ikushima, H., et al., Autocrine TGF-β signaling maintains tumorigenicity of glioma-initiating cells through Sry-related HMG-box factors. Cell Stem Cell, 2009. 5(5): p. 504-14.
80. Fink, S.P., et al., TGF-β-induced nuclear localization of Smad2 and Smad3 in Smad4 null cancer cell lines. Oncogene, 2003. 22(9): p. 1317-23.
81. Lu, J., et al., β-Galactoside alpha2,6-sialyltranferase 1 promotes transforming growth factor-β-mediated epithelial-mesenchymal transition. J Biol Chem, 2014. 289(50): p. 34627-41.
82. Schultz, M.J., A.F. Swindall, and S.L. Bellis, Regulation of the metastatic cell phenotype by sialylated glycans. Cancer Metastasis Rev, 2012. 31(3-4): p. 501-18.
83. Munkley, J., The Role of Sialyl-Tn in Cancer. Int J Mol Sci, 2016. 17(3): p. 275.
84. Zhang, T., et al., Differential O- and Glycosphingolipid Glycosylation in Human Pancreatic Adenocarcinoma Cells With Opposite Morphology and Metastatic Behavior. Front Oncol, 2020. 10: p. 732.
85. Guan, F., K. Handa, and S.I. Hakomori, Specific glycosphingolipids mediate epithelial-to-mesenchymal transition of human and mouse epithelial cell lines. Proc Natl Acad Sci U S A, 2009. 106(18): p. 7461-6.
86. Kim, S.J., et al., Ganglioside GM3 participates in the TGF-β1-induced epithelial-mesenchymal transition of human lens epithelial cells. Biochem J, 2013. 449(1): p. 241-51.
87. de Sousa Abreu, R., et al., Global signatures of protein and mRNA expression levels. Mol Biosyst, 2009. 5(12): p. 1512-26.

88. Maier, T., M. Guell, and L. Serrano, Correlation of mRNA and protein in complex biological samples. FEBS Lett, 2009. 583(24): p. 3966-73.
89. Inokuchi, J.-i., et al., Inhibition of Experimental Metastasis of Murine Lewis Lung Carcinoma by an Inhibitor of Glucosylceramide Synthase and Its Possible Mechanism of Action. Cancer Res, 1990. 50(20): p. 6731-6737.
90. Kovbasnjuk, O., et al., The glycosphingolipid globotriaosylceramide in the metastatic transformation of colon cancer. Proc Natl Acad Sci U S A, 2005. 102(52): p. 19087-92.
91. Falguieres, T., et al., Human colorectal tumors and metastases express Gb3 and can be targeted by an intestinal pathogen-based delivery tool. Mol Cancer Ther, 2008. 7(8): p. 2498-508.
92. Stimmer, L., et al., Human breast cancer and lymph node metastases express Gb3 and can be targeted by STxB-vectorized chemotherapeutic compounds. BMC Cancer, 2014. 14: p. 916.
93. Geyer, P.E., et al., Gastric Adenocarcinomas Express the Glycosphingolipid Gb3/CD77: Targeting of Gastric Cancer Cells with Shiga Toxin B-Subunit. Mol Cancer Ther, 2016. 15(5): p. 1008-17.
94. Storck, W., et al., Shiga toxin glycosphingolipid receptor expression and toxin susceptibility of human pancreatic ductal adenocarcinomas of differing origin and differentiation. Biol Chem, 2012. 393(8): p. 785-99.
95. Bagati, A., et al., Integrin αvβ6-TGFβ-SOX4 Pathway Drives Immune Evasion in Triple-Negative Breast Cancer. Cancer Cell, 2021. 39(1): p. 54-67 e9.
96. van de Wetering, M., et al., Specific inhibition of gene expression using a stably integrated, inducible small-interfering-RNA vector. EMBO Rep, 2003. 4(6): p. 609-15.
97. Liu, Y., et al., Transforming growth factor-β (TGF-β)-mediated connective tissue growth factor (CTGF) expression in hepatic stellate cells requires Stat3 signaling activation. J Biol Chem, 2013. 288(42): p. 30708-19.
98. Wang, S.E., et al., Transforming growth factor β induces clustering of HER2 and integrins by activating Src-focal adhesion kinase and receptor association to the cytoskeleton. Cancer Res, 2009. 69(2): p. 475-82.
99. Varadaraj, A., et al., TGF-β triggers rapid fibrillogenesis via a novel TβRII-dependent fibronectin-trafficking mechanism. Mol Biol Cell, 2017. 28(9): p. 1195-1207.
100. To, C., et al., The synthetic triterpenoid 2-cyano-3,12-dioxooleana-1,9-dien-28-oic acid-imidazolide alters transforming growth factor β-dependent signaling and cell migration by affecting the cytoskeleton and the polarity complex. J Biol Chem, 2008. 283(17): p. 11700-13.

101. Edlund, S., et al., Transforming growth factor-β-induced mobilization of actin cytoskeleton requires signaling by small GTPases Cdc42 and RhoA. Mol Biol Cell, 2002. 13(3): p. 902-14.
102. Elsasser, H.P., et al., Establishment and characterisation of two cell lines with different grade of differentiation derived from one primary human pancreatic adenocarcinoma. Virchows Arch B Cell Pathol Incl Mol Pathol, 1992. 61(5): p. 295-306.
103. Zhang, L., et al., USP4 is regulated by AKT phosphorylation and directly deubiquitylates TGF-β type I receptor. Nat Cell Biol, 2012. 14(7): p. 717-26.
104. Ren, J., et al., Invasive Behavior of Human Breast Cancer Cells in Embryonic Zebrafish. J Vis Exp, 2017(122).
105. Madunic, K., et al., Colorectal cancer cell lines show striking diversity of their O-glycome reflecting the cellular differentiation phenotype. Cell Mol Life Sci, 2020.
106. Karlsson, N.G., et al., Negative ion graphitised carbon nano-liquid chromatography/mass spectrometry increases sensitivity for glycoprotein oligosaccharide analysis. Rapid Commun Mass Spectrom, 2004. 18(19): p. 2282-92.
107. Karlsson, N.G., B.L. Schulz, and N.H. Packer, Structural determination of neutral O-linked oligosaccharide alditols by negative ion LC-electrospray-MSn. J Am Soc Mass Spectrom, 2004. 15(5): p. 659-72.
108. Ceroni, A., et al., GlycoWorkbench: a tool for the computer-assisted annotation of mass spectra of glycans. J Proteome Res, 2008. 7(4): p. 1650-9.
109. Cooper, C.A., E. Gasteiger, and N.H. Packer, GlycoMod--a software tool for determining glycosylation compositions from mass spectrometric data. Proteomics, 2001. 1(2): p. 340-9.